

# Weak, frictionally unstable input sediments explain shallow seismogenesis at the north Sumatran subduction zone

Katja Stanislawski<sup>1</sup>, Andre Hüpers<sup>1</sup>, Åke Fagereng<sup>2</sup>, and Matt J. Ikari<sup>1,\*</sup>

<sup>1</sup>MARUM (Center for Marine Environmental Sciences), and Faculty of Geosciences, University of Bremen, D-28359 Bremen, Germany

<sup>2</sup>School of Earth and Environmental Sciences, Cardiff University, Cardiff CF10 3AT, UK

## ABSTRACT

The cause of unexpectedly shallow seismic slip during the 2004 Sumatra-Andaman earthquake, which resulted in a devastating tsunami, is still under debate. One hypothesis is that diagenetic strengthening of décollement-forming input sediments prior to subduction allows shallow seismogenic behavior. We tested this hypothesis by measuring the frictional behavior of input sediments, sampled offshore northern Sumatra during International Ocean Discovery Program (IODP) Expedition 362, in single-direct shear experiments. The input sediments that have been correlated with the north Sumatra proto-décollement horizon are frictionally unstable, indicating a seismogenic shallow décollement. These sediments are also frictionally weak, which deviates from expected friction systematics but means that diagenetic strengthening is not required. Our observations indicate that threshold concentrations of amorphous silica ( $\geq 11$  wt%), palagonite rims on glass fragments, and feldspar interspersed within weak, smectite-bearing sediments entering the north Sumatra subduction zone may cause the incoming sediments to be frictionally unstable before subduction. This instability led to the unexpectedly shallow coseismic slip during the 2004 Sumatra-Andaman earthquake and may be valuable information for hazard assessments of other subduction margins.

## INTRODUCTION

During the 2004  $M_w$  9.2 Sumatra-Andaman subduction zone earthquake, the largest seismic slip initiated offshore north Sumatra, and the rupture propagated northward along strike toward the Andaman Islands (Fig. 1A; Ammon et al., 2005; Lay et al., 2005). Most slip models agree on a large amount of shallow coseismic slip, suggesting that the trenchmost area of the fault offshore northern Sumatra participated in the mainshock (e.g., Lay et al., 2005; Banerjee et al., 2007; Rhie et al., 2007). The result was a large-magnitude earthquake and devastating tsunami, making it imperative to examine how this could occur.

Diagenetic processes such as quartz precipitation, smectite-illite transformation, and pore pressure dissipation in the proto-décollement have been suggested as the cause of the shallow seismogenesis at Sumatra (Hüpers et al., 2017),


by strengthening the sediments and inducing unstable sliding (Moore and Saffer, 2001; Trüner et al., 2015). This view contrasts with the seismogenic zone model, where completion of these processes is only expected after subduction to depths of several kilometers (5–10 km; Hyndman et al., 1997). Although the hypothesis of strengthened input material by Hüpers et al. (2017) is consistent with sediment strengthening by burial-related dewatering and lithification (Gulick et al., 2011; Geersen et al., 2013; Stevens et al., 2021), friction data are necessary for verification.

We performed laboratory friction experiments, combined with mineral composition and porosity measurements, on input sediments recovered between 1250 and 1360 m below seafloor (mbsf) at Site U1480, drilled during International Ocean Discovery Program (IODP) Expedition 362 (McNeill et al., 2017). The site is located 225 km seaward of the north Sumatran deformation front, where the largest coseismic slip occurred during the mainshock of the 2004 earthquake. The target depth interval comprises lithostratigraphic unit

III, which has been correlated with the seaward extension of a high-amplitude negative-polarity (HANP) seismic reflector interpreted to represent the proto-décollement horizon (Fig. 1B; Dean et al., 2010). In the absence of available fault zone material, subduction zone input sediments provide key information on the shallow megathrust (Underwood, 2007; Stanislawski et al., 2022); therefore, we evaluated the mechanical characteristics of the proto-décollement sediments and their implications for the possibility of a shallow seismogenic zone.

## EXPERIMENTAL METHODS

We performed laboratory friction experiments on eight different samples from the targeted depth interval in a GIESA RS5 single-direct shear device at room temperature, under in situ effective normal stresses, and samples saturated with simulated seawater (Fig. S1 in the Supplemental Material<sup>1</sup>; e.g., Stanislawski et al., 2022). X-ray diffraction (XRD) measurements were made postexpedition following the double-identification method of Vogt et al. (2002), showing that the noncalcareous samples consisted of 28–64 wt% phyllosilicate minerals, 13–36 wt% quartz + feldspar, and 0–20 wt% nearly amorphous silica; the calcareous samples had a calcite content of >90 wt%. The samples were tested as powders (grain size <125  $\mu\text{m}$ ) and where possible as intact specimens with no predefined shear plane (Fig. 2). Powdered samples were mixed with simulated seawater and consolidated at their estimated in situ effective normal stress ( $\sim 11$ –14 MPa) for >20 h, after the change in thickness became negligible, indicating full pore-pressure dissipation. In each experiment, the samples were sheared in three successive phases: (1) at a constant velocity  $V$  of 10  $\mu\text{m/s}$  for  $\sim 5$  mm sample displacement ( $x$ ) to establish a steady-state coefficient of sliding friction

Matt J. Ikari  <https://orcid.org/0000-0002-8164-411X>  
\*mikari@marum.de

<sup>1</sup>Supplemental Material. Extended methods description, additional data figures, microstructural images, and description of the microstructural images. Please visit <https://doi.org/10.1130/GEOLOG.S.28299347> to access the supplemental material; contact [editing@geosociety.org](mailto:editing@geosociety.org) with any questions.

CITATION: Stanislawski, K., et al., 2025, Weak, frictionally unstable input sediments explain shallow seismogenesis at the north Sumatran subduction zone: *Geology*, v. XX, p. , <https://doi.org/10.1130/G52910.1>

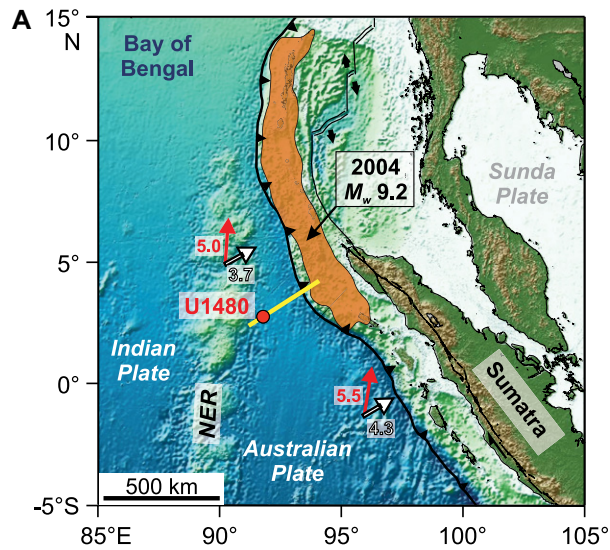


Figure 1. (A) Map of northern Sumatra subduction zone, showing rupture zone of 2004 earthquake (orange patch) and location of International Ocean Discovery Program (IODP) Site U1480 (red dot). Red and white arrows indicate convergence and subduction vectors (cm/yr). Yellow line shows location of seismic lines BGR06-102 and BGR06-101 in panel B. (B) Seismic lines BGR06-102 and BGR06-101. Red dashed line marks high-amplitude negative-polarity (HANP) reflector interpreted to be proto-décollement. Blue line indicates base of trench wedge sediments. NER—Ninety East Ridge. Figure is modified from Hüpers et al. (2017) and McNeill et al. (2017).

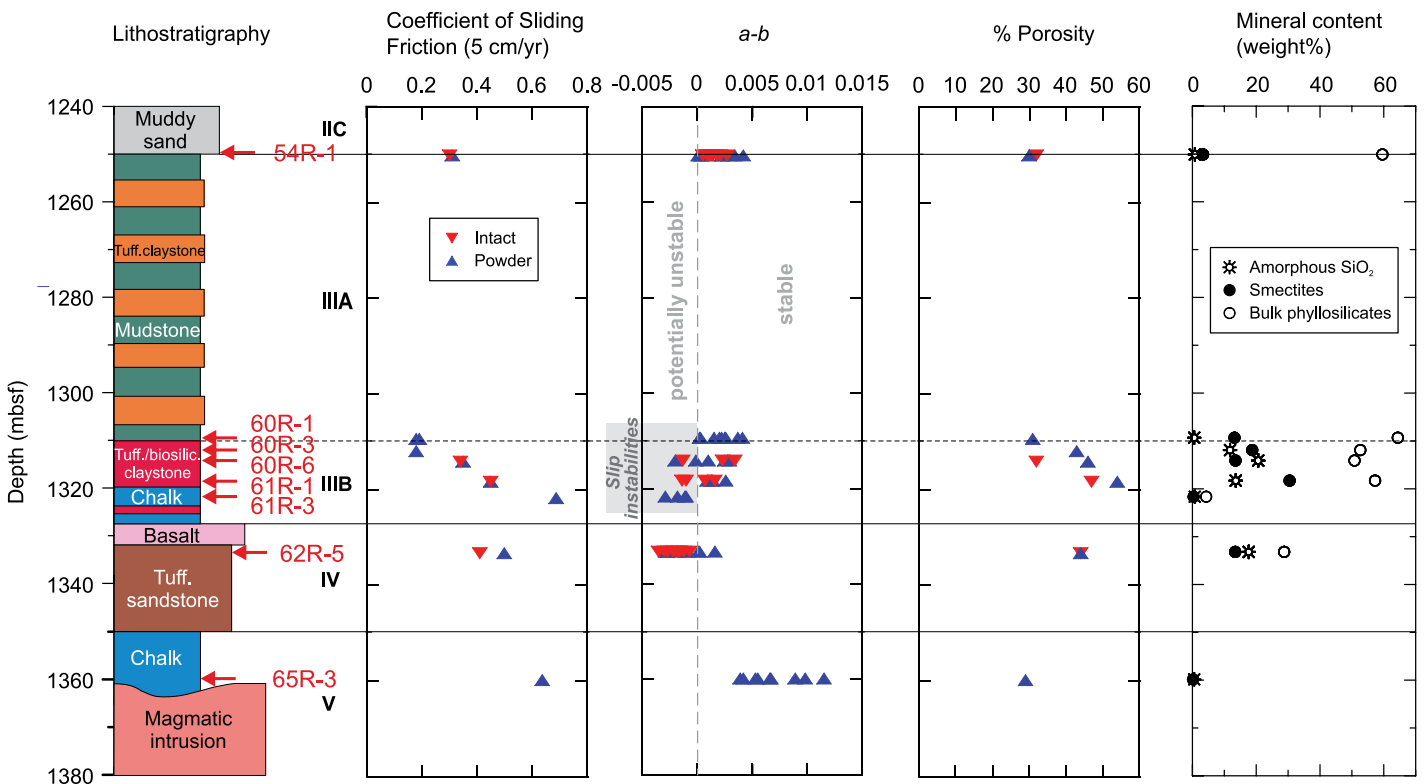
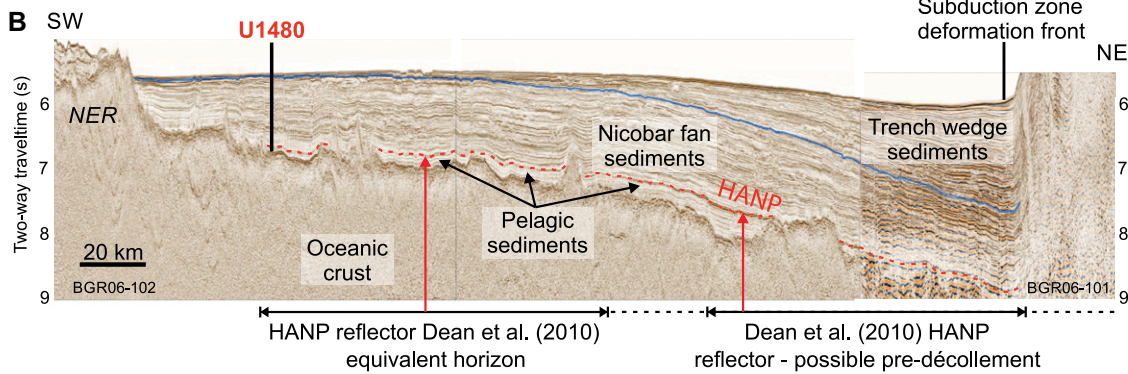


Figure 2. Lithostratigraphic column (modified from McNeill et al., 2017; mbsf—meters below seafloor; tuff.—tuffaceous), coefficient of sliding friction  $\mu$  from phase of plate rate (5 cm/yr) shearing, rate-dependent friction parameter  $a-b$  for all sliding velocities, porosity, and specific mineral contents for tested samples.

tion ( $\mu$ ), (2) at a slow velocity (5.3 cm/yr) similar to the plate convergence rate for  $x = 2$  mm, and (3) in a sequence of threefold increasing velocity steps in the range of 0.003–30  $\mu\text{m/s}$  for  $x = 0.7$  mm per velocity step (Fig. S1). The apparent coefficient of sliding friction ( $\mu$ ) was calculated from the ratio of the continuously measured shear stress to the applied effective normal stress. Cohesion was therefore included in  $\mu$ , but it was also measured separately (Fig. S2). The frictional response to a velocity step was quantified by inverse modeling using the MATLAB code RSFit3000 to obtain the velocity-dependent friction parameter  $a-b = \Delta\mu/\Delta\ln V$  (Skarbek and Savage, 2019) (Fig. 2; see also Supplemental Material). Positive values of  $a-b$  indicate velocity-strengthening behavior associated with stable slip, whereas negative values indicate velocity-weakening behavior that, in combination with sufficiently compliant fault surroundings, is required for slip instability and favors coseismic slip (Dieterich, 1981; Marone, 1998; Scholz, 1998). Sample porosity was measured postexpedition on seawater-saturated consolidated powders by determining the change in mass after oven drying for  $\geq 24$  h at 105 °C (Supplemental Material). Postmortem samples were imaged by scanning electron microscopy (SEM) in backscatter mode, and in some cases by energy-dispersive X-ray spectroscopy (EDS).

## MECHANICAL AND PHYSICAL PROPERTIES

Steady-state coefficients of sliding friction measured at plate-rate shearing velocity ranged between  $\mu = 0.18$ –0.69 (Fig. 2). Friction coefficients from the initial (run-in) phase at 10  $\mu\text{m/s}$

were slightly lower (0.14–0.62) and followed the same pattern with depth as those measured at the plate rate (Fig. S3). The highest value was found for the powdered calcareous samples, and the lowest values were found for powdered mudstone from 1309 mbsf (core sample 60R-1) and red silty clay with ash from 1312 mbsf (60R-3). Minor lithification is indicated by cohesion values of 190–990 kPa (Fig. S2).

Our measurements of the parameter  $a-b$  ranged from  $-0.003$  to  $+0.012$  (Fig. 2). The mudstone from 1250 mbsf (54R-1) and chalk from 1360 mbsf (65R-3) exhibited strictly velocity-strengthening behavior and stable sliding; all other tested samples, which were collected within the depth interval of 1309–1333 mbsf, showed some velocity-weakening and/or stick-slip sliding behavior, which is direct evidence of frictional instability (Figs. 2 and 3A). The stress drops of recorded slip instabilities ranged from 5 to 665 kPa and generally correlated with the slip event speed increase, quantified as the ratio of the average slip velocity  $V$  to the driving velocity  $V_{ip}$  (Fig. 3C), where the average velocity was calculated from the slip during the stress drop and the duration of the stress drop. Exceptions to this observed trend were some instabilities in the ash-bearing silty clay from 1322 mbsf (60R-3). Many of the events were instances of slow slip, with  $V \sim 1$  order of magnitude faster than  $V_{ip}$ .

Porosities of the powdered samples were relatively high (43%–54%) in the depth interval from 1312 to 1333 mbsf (no measurement could be made for the chalk at 1322 mbsf), which coincided with the interval in which velocity weakening and unstable sliding were observed. Whereas the porosities of the other samples

(29%–32%) fell onto the normal compaction trend (Hüpers et al., 2017), the high porosities of this distinct depth interval clearly deviated from the trend.

## FRICIONAL INSTABILITY OF PROTO-DÉCOLLEMENT SEDIMENTS

Because we observed instances of velocity-weakening behavior and/or stick-slip instabilities under in situ conditions for all tested samples from lithostratigraphic units III and IV (Figs. 2 and 3), the Sumatra input sediments that likely host the shallow décollement are interpreted to be frictionally unstable prior to subduction. In particular, the red silty clay with ash from 1312 mbsf was frictionally unstable from near the plate rate up to the maximum velocity tested in this study (Fig. 3). Given that this was also the weakest sample we tested ( $\mu_s = 0.18$ ; Fig. 2), this lithology may be the locus of décollement formation and capable of coseismic slip at shallow depths. Also notable were the intact samples of tuffaceous sandstone from 1333 mbsf (unit IV), which exhibited velocity-weakening behavior from the plate rate through the entire tested velocity range, and the chalk (61R-3) from 1322 mbsf (unit III), which failed in stick-slip instabilities with relatively large stress drops when driven at the plate rate (Fig. 3). Although samples 60R-6 and 61R-1 (unit III) also exhibited (potentially) unstable sliding behavior, it occurred when the driving velocity was at least one order of magnitude faster than the plate rate (Fig. 3A). If these sediments were to host plate-boundary slip, they would need to be perturbed by a deeper-seated earthquake or a slow slip event. Collectively, our findings suggest that the seismogenic zone at Sumatra has no

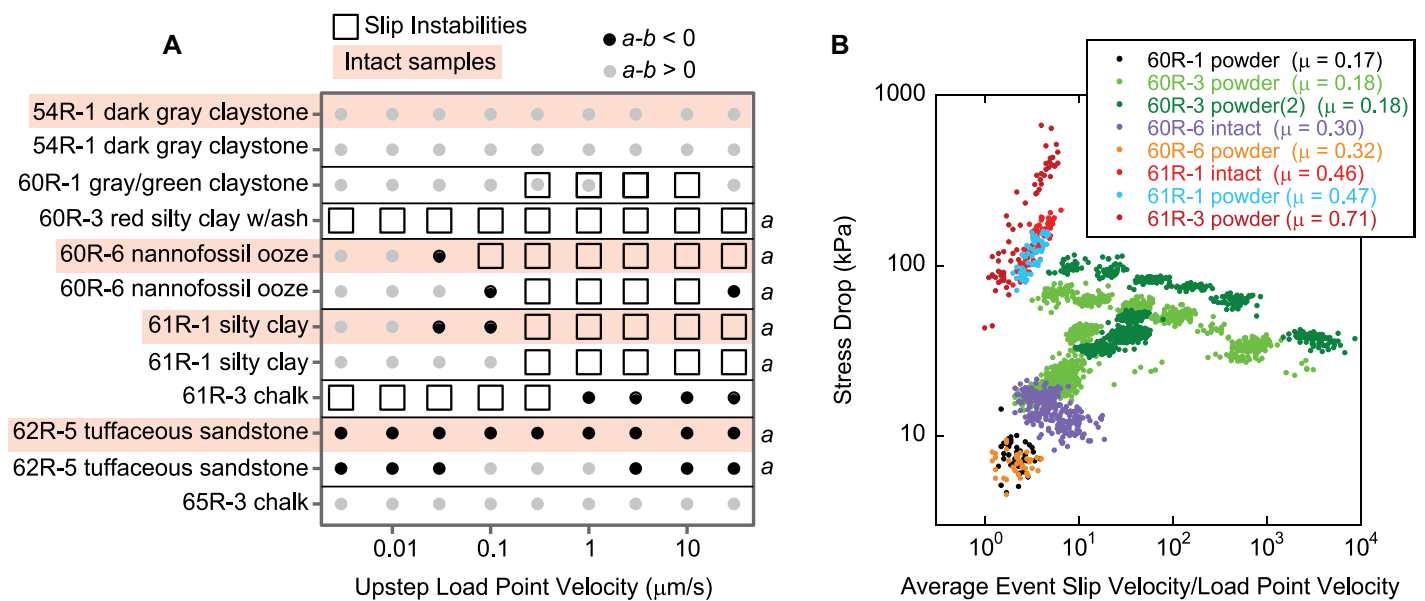


**Figure 3. (A) Polarity of friction velocity dependence ( $a-b$ ) and occurrences of slip instabilities as function of up-step driving velocity. Both experiments (KS067, KS132) are shown for 60R-1, resulting in some overlapping symbols. Intact samples are shown with red shading; a—sample contains amorphous  $\text{SiO}_2$  (B) Stress drop as function of average stick-slip event velocity, normalized to load point velocity during slip instabilities.**

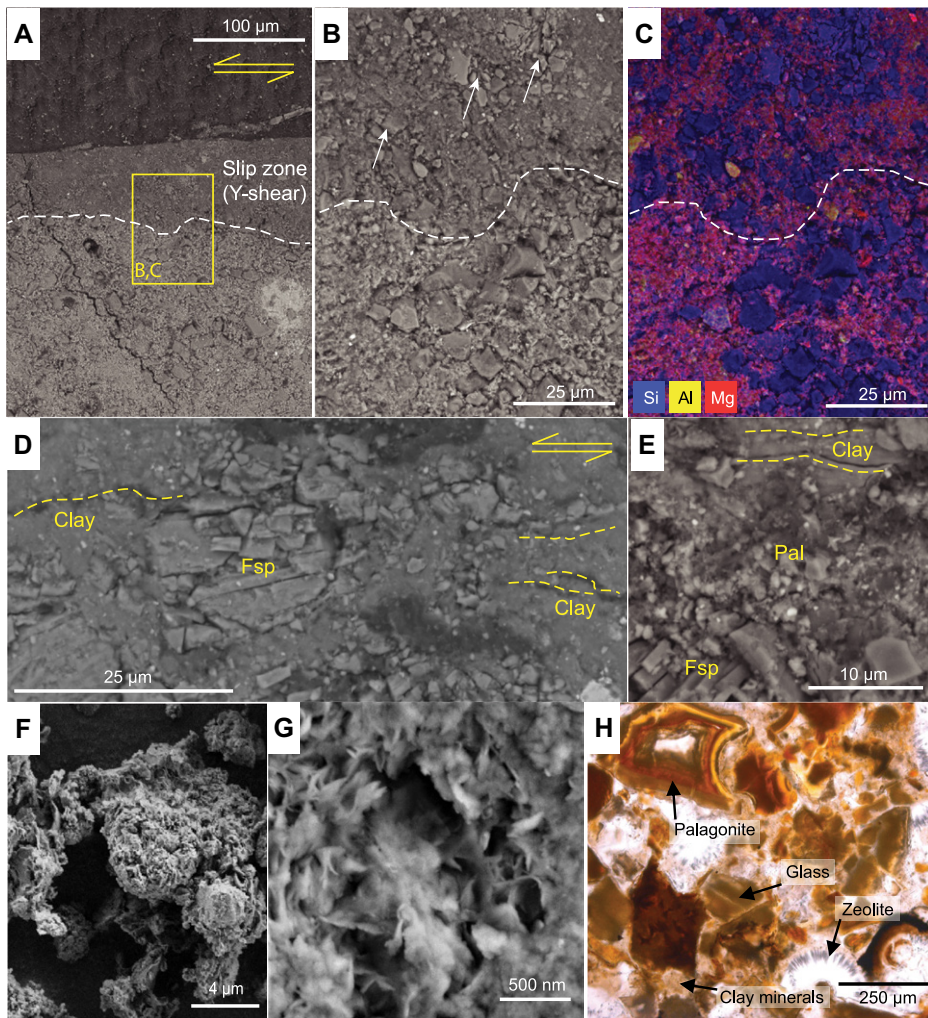


**Figure 4.** (A) Backscattered electron (BSE) image of wide fine-grained *Y* shear along slipping zone (above white dashed line) in sample 61R-1. Yellow box shows location of close-up image in B and energy-dispersive X-ray spectroscopy (EDS) map in C. (B–C) BSE and EDS images of fragmented feldspar and palagonite (highlighted by white arrows in B) scattered in smectite-rich gouge. In C, feldspar appears as light blue, palagonite as dark blue, and smectite-rich gouge as red/purple. (D–E) BSE images of deformed sample 62R-5, showing (D) fractured feldspar (Fsp) sheared out within clay-rich gouge with poorly developed fabric (dashed yellow lines), and (E) fragmented feldspar bordered by very fine palagonite (Pal) in weakly foliated clay. (F–G) BSE images of (F) clay-coated aggregates of powdered undeformed sample 60R-6, and (G) flakes of clay and powdery palagonite in powdered undeformed sample 62R-5. (H) Optical, plane-light photomicrograph of intact undeformed sample 60R-1, showing individual mineral components including palagonite and clay.

updip limit, and these results offer an explanation for the seismogenic slip near the trench during the Sumatra-Andaman earthquake.

#### CAUSE OF FRICTIONAL INSTABILITY

Although our tested Sumatra sediment samples followed the generally expected systematics of increasing frictional strength with decreasing *a-b*, our data were shifted so that the (potentially) frictionally unstable materials were also frictionally weak ( $\mu_s = 0.17\text{--}0.47$ ; Figs. 2 and 3B), contrary to the expectation that velocity weakening and slip instability should only occur in relatively strong sediments ( $\mu > \sim 0.5$ ; Beeler, 2007; Ikari et al., 2016). The unusual combination of frictional weakness and insta-

bility in the Sumatra input sediments is difficult to explain. We note that our microstructural images of sheared samples show a reduced grain size and local grain-scale fracturing, implying a cataclastic process. Deformation was localized in  $>100\text{-}\mu\text{m}$ -thick zones parallel to the shear plane, essentially *Y* shears (e.g., Figs. 4A–4C). In these shears, clays made up a matrix surrounding stronger, fragmented clasts of feldspar, quartz, and palagonite (Fig. 4). Locally, there was a weakly developed foliation in the clay matrix (Figs. 4D–4E), but this was neither interconnected nor continuous along the sampled shear features (e.g., Fig. 4D).

In quartzofeldspathic sediments undergoing cataclastic deformation, one may expect a

Byerlee (1978) friction value of  $\sim 0.6$  and the development of *Y* shears associated with stick-slip or velocity-weakening behavior (Beeler, 1996; Logan et al., 1992; Niemeijer and Spiers, 2005). Clay minerals, especially smectite, are expected to substantially lower the strength of the sediments and cause velocity strengthening (Morrow et al., 1992; Ikari et al., 2009), but this is usually associated with the development of a continuous, interconnected phyllosilicate fabric (Bos et al., 2000; Colletini et al., 2009; Haines et al., 2013). Our samples contained abundant clay (up to 64 wt% total phyllosilicates) and significant smectite (up to 30 wt%) (Fig. 2), which developed a matrix in the cataclastic *Y* shears (Figs. 4A–4E). Importantly, however, the clays in the *Y* shears did not develop a continuous fabric, allowing stronger grains of feldspar, quartz, and also palagonite to interact during shear (Figs. 4D–4H), leading to velocity-weakening or unstable frictional behavior. One could speculate that if the sediments we tested were deformed to greater strains, a through-going, foliated clay fabric may eventually form, and the samples would become weaker as well as velocity strengthening.

Our observations of elevated amorphous silica content, elevated smectite content, and higher porosity in samples that exhibited velocity-weakening friction or slip instabilities (Fig. 2) suggest the potential importance of palagonite. Palagonite is a product of the aqueous alteration of basaltic volcanic glass (Singer and Banin, 1990; Stroncik and Schmincke, 2002). It is a “composite” substance that typically includes the reaction products smectite and zeolite (and in some cases, carbonate or oxide minerals), but it also includes poorly crystalline precursors of smectite. Palagonite is also less dense than the original glass, and it has an internal porosity of up to 9% (Singer and Banin, 1990). Shipboard smear slide analyses by Hüpers et al. (2017) identified palagonite along with a minor component of biogenic opal in Sumatra input sediments. In our samples, palagonite was identified by XRD data combined with optical and SEM images showing the characteristic appearance as rims of clays and zeolite on glass fragments (Fig. 4H). We speculate that the rind-core structure of palagonite may play a mechanical role, as the thin clay rinds may be sheared by allowing the amorphous glass particles to act as contact asperities. To our knowledge, data from dedicated friction experiments on palagonite are not currently available. To test the properties of the opal component, we performed an additional experiment on a powdered sample of pure biogenic opal from Humboldt County, Nevada, USA, at an effective normal stress of 13 MPa. That experiment revealed a friction coefficient of 0.67 (at 5 cm/yr) and slip instabilities throughout the entire test.

Our combined observations of elevated amorphous silica and smectite contents,

increased porosity, and SEM imaging of the proto-décollement sediments suggest that cataclasis of palagonite, feldspar, and quartz in a discontinuous clay matrix with poorly developed fabric may be responsible for weak and unstable frictional behavior, with palagonite rims on glass fragments playing an important role. These results provide an explanation for shallow earthquake slip at Sumatra and bear important implications for hazards in other subduction zones where the incoming sediments contain altered volcanic glass, since volcanic ash (as the source of palagonite; Underwood, 2007; White et al., 2011) and opal (Rea and Ruff, 1996) are commonly found in the sedimentary inputs to many subduction zones.

#### ACKNOWLEDGMENTS

This research used samples and/or data provided by the International Ocean Discovery Program. This work was supported by the European Research Council (ERC) under the European Union's Horizon 2020 research and innovation programme grant 714430 to M. Ikari and by UK Research and Innovation (UKRI) Frontier Research grant ref. EP/Y024672/1 to Å. Fagereng. We thank John Bedford and Li-Wei Kuo for helpful comments on the manuscript. All data are available from the Pangaea data publisher for earth and environmental science: <https://doi.pangaea.de/10.1594/PANGAEA.966244>.

#### REFERENCES CITED

Ammon, C.J., Ji, C., Thio, H.-K., Robinson, D., Ni, S., Hjørleifsdóttir, V., Kanamori, H., Lay, T., Das, S., Helmberger, D., Ichinose, G., Polet, J., and Wald, D., 2005, Rupture process of the 2004 Sumatra-Andaman earthquake: *Science*, v. 308, p. 1133–1139, <https://doi.org/10.1126/science.1112260>.

Banerjee, P., Pollitz, F., Nagarajan, B., and Bürgmann, R., 2007, Coseismic slip distributions of the 26 December 2004 Sumatra-Andaman and 28 March 2005 Nias earthquakes from GPS static offsets: *Bulletin of the Seismological Society of America*, v. 97, p. S86–S102, <https://doi.org/10.1785/0120050609>.

Beeler, N.M., 1996, Frictional behavior of large-displacement experimental faults: *Journal of Geophysical Research*, v. 110, p. 8697–8715, <https://doi.org/10.1029/96JB00411>.

Beeler, N.M., 2007, Laboratory-observed faulting in intrinsically and apparently weak materials, *in* Dixon, T.H., and Moore, J.C., eds., *The Seismogenic Zone of Subduction Thrust Faults*: New York, Columbia University Press, p. 370–449, <https://doi.org/10.7312/dixo13866-013>.

Bos, B., Peach, C.J., and Spiers, C.J., 2000, Frictional-viscous flow of simulated fault gouge caused by the combined effects of phyllosilicates and pressure solution: *Tectonophysics*, v. 327, p. 173–194, [https://doi.org/10.1016/S0040-1951\(00\)00168-2](https://doi.org/10.1016/S0040-1951(00)00168-2).

Byerlee, J.D., 1978, Friction of rocks: *Pure and Applied Geophysics*, v. 116, p. 615–626, <https://doi.org/10.1007/BF00876528>.

Colletinni, C., Niemeijer, A., Viti, C., and Marone, C., 2009, Fault zone fabric and fault weakness: *Nature*, v. 462, p. 907–910, <https://doi.org/10.1038/nature08585>.

Dean, S.M., McNeill, L.C., Henstock, T.J., Bull, J.M., Gulick, S.P.S., Austin, J.A., Jr., Bangs, N.L.B., Djajadihardja, Y.S., and Permana, H., 2010, Contrasting décollement and prism properties over the Sumatra 2004–2005 earthquake rupture boundary: *Science*, v. 329, p. 207–210, <https://doi.org/10.1126/science.1189373>.

Dieterich, J.H., 1981, Constitutive properties of faults with simulated gouge, *in* Carter, N.L., Friedman, M., Logan, J.M., and Stearns, D.W., eds., *Mechanical Behavior of Crustal Rocks: The Handin Volume*: American Geophysical Union Geophysical Monograph 24, p. 103–120, <https://doi.org/10.1029/GM024p0103>.

Geersen, J., McNeill, L., and Henstock, T.J., 2013, The 2004 Aceh-Andaman earthquake: Early clay dehydration controls shallow seismic rupture: *Geochemistry, Geophysics, Geosystems*, v. 14, p. 3315–3323, <https://doi.org/10.1002/ggge.20193>.

Gulick, S.P.S., Austin, J.A., Jr., McNeill, L.C., Bangs, N.L.B., Martin, K.M., Henstock, T.J., Bull, J.M., Dean, S., Djajadihardja, Y.S., and Permana, H., 2011, Updip rupture of the 2004 Sumatra earthquake extended by thick indurated sediments: *Nature Geoscience*, v. 4, p. 453–456, <https://doi.org/10.1038/ngeo1176>.

Haines, S.H., Kaproth, B., Marone, C., Saffer, D., and van der Pluijm, B., 2013, Shear zones in clay-rich fault gouge: A laboratory study of fabric development and evolution: *Journal of Structural Geology*, v. 51, p. 206–225, <https://doi.org/10.1016/j.jsg.2013.01.002>.

Hüpers, A., et al., 2017, Release of mineral-bound water prior to subduction tied to shallow seismogenic slip off Sumatra: *Science*, v. 356, p. 841–844, <https://doi.org/10.1126/science.aal3429>.

Hyndman, R.D., Yamano, M., and Oleskevich, D.A., 1997, The seismogenic zone of subduction thrust faults: *The Island Arc*, v. 6, p. 244–260, <https://doi.org/10.1111/j.1440-1738.1997.tb00175.x>.

Ikari, M.J., Saffer, D.M., and Marone, C., 2009, Frictional and hydrologic properties of clay-rich fault gouge: *Journal of Geophysical Research*, v. 114, B05409, <https://doi.org/10.1029/2008JB006089>.

Ikari, M.J., Carpenter, B.M., and Marone, C., 2016, A microphysical interpretation of rate- and state-dependent friction for fault gouge: *Geochemistry, Geophysics, Geosystems*, v. 17, p. 1660–1677, <https://doi.org/10.1002/2016GC006286>.

Lay, T., Kanamori, H., Ammon, C.J., Nettles, M., Ward, S.N., Aster, R.C., Beck, S.L., Bilek, S.L., Brudzinski, M.R., Butler, R., Deshon, H.R., Ekström, G., and Sipkin, S., 2005, The great Sumatra-Andaman earthquake of 26 December 2004: *Science*, v. 308, p. 1127–1133, <https://doi.org/10.1126/science.1112250>.

Logan, J.M., Dengo, C.A., Higgs, N.G., and Wang, Z.Z., 1992, Fabrics of experimental fault zones: Their development and relationship to mechanical behavior: *International Geophysics*, v. 51, p. 33–67, [https://doi.org/10.1016/S0074-6142\(08\)62814-4](https://doi.org/10.1016/S0074-6142(08)62814-4).

Marone, C., 1998, Laboratory-derived friction laws and their application to seismic faulting: *Annual Review of Earth and Planetary Sciences*, v. 26, p. 643–696, <https://doi.org/10.1146/annurev.earth.26.1.643>.

McNeill, L.C., et al., 2017, Expedition 362 summary, *in* McNeill, L.C., Dugan, B., Petronotis, K.E., and the Expedition 362 Scientists, *Sumatra Subduction Zone: Proceedings of the International Ocean Discovery Program, Volume 362*: College Station, Texas, International Ocean Discovery Program, <https://doi.org/10.14379/iodp.proc.362.101.2017>.

Moore, J.C., and Saffer, D.M., 2001, Updip limit of the seismogenic zone beneath the accretionary prism of Southwest Japan: An effect of diagenetic to low-grade metamorphic processes and increasing effective stress: *Geology*, v. 29, p. 183–186, [https://doi.org/10.1130/0091-7613\(2001\)029<0183:ULO TSZ>2.0.CO;2](https://doi.org/10.1130/0091-7613(2001)029<0183:ULO TSZ>2.0.CO;2).

Morrow, C.A., Moore, D.E., and Lockner, D.A., 1992, Frictional strength and the effective pressure law of montmorillonite and illite clays: *International*

*Geophysics*, v. 51, p. 69–88, [https://doi.org/10.1016/S0074-6142\(08\)62815-6](https://doi.org/10.1016/S0074-6142(08)62815-6).

Niemeijer, A.R., and Spiers, C.J., 2005, Influence of phyllosilicates on fault strength in the brittle-ductile transition: Insights from rock analogue experiments, *in* Bruhn, D., and Burlini, L., eds., *High-Strain Zones: Structure and Physical Properties*: Geological Society, London, Special Publications, v. 245, p. 303–327, <https://doi.org/10.1144/GSL.SP.2005.245.01.15>.

Rea, D.K., and Ruff, L.J., 1996, Composition and mass flux of sediment entering the world's subduction zones: Implications for global sediment budgets, great earthquakes and volcanism: *Earth and Planetary Science Letters*, v. 140, p. 1–12, [https://doi.org/10.1016/0012-821X\(96\)00036-2](https://doi.org/10.1016/0012-821X(96)00036-2).

Rhie, J., Dreger, D., Bürgmann, R., and Romanowicz, B., 2007, Slip of the 2004 Sumatra-Andaman earthquake from joint inversion of long-period global seismic waveforms and GPS static offsets: *Bulletin of the Seismological Society of America*, v. 97, p. S115–S127, <https://doi.org/10.1785/0120050620>.

Scholz, C.H., 1998, Earthquakes and friction laws: *Nature*, v. 391, p. 37–42, <https://doi.org/10.1038/34097>.

Singer, A., and Banin, A., 1990, Characteristics and mode of palagonite—A review, *in* Farmer, V.C., and Tardy, Y., eds., *Proceedings of the 9th International Clay Conference, Strasbourg, 1989, Volume IV: Clays in Sediments. Diagenesis and Hydrothermalism*: Sciences Géologiques, Bulletin e Mémoires 88, p. 173–181.

Skarbak, R.M., and Savage, H.M., 2019, RSFit3000: A MATLAB GUI-based program for determining rate and state frictional parameters from experimental data: *Geosphere*, v. 15, p. 1665–1676, <https://doi.org/10.1130/GES02122.1>.

Stanislawski, K., Roesner, A., and Ikari, M.J., 2022, Implications for megathrust slip behavior and pore pressure at the shallow northern Cascadia subduction zone from laboratory friction experiments: *Earth and Planetary Science Letters*, v. 578, <https://doi.org/10.1016/j.epsl.2021.117297>.

Stevens, D.E., Henstock, T.J., and McNeill, L.C., 2021, Evolution of the thermal and dehydration state of sediments entering the North Sumatra subduction zone: *Geochemistry, Geophysics, Geosystems*, v. 22, <https://doi.org/10.1029/2020GC009306>.

Stroncik, N.A., and Schmincke, H.-U., 2002, Palagonite—A review: *International Journal of Earth Sciences*, v. 91, p. 680–697, <https://doi.org/10.1007/s00531-001-0238-7>.

Trütner, S., Hüpers, A., Ikari, M.J., Yamaguchi, A., and Kopf, A.J., 2015, Lithification facilitates frictional instability in argillaceous subduction zone sediments: *Tectonophysics*, v. 665, p. 177–185, <https://doi.org/10.1016/j.tecto.2015.10.004>.

Underwood, M.B., 2007, Sediment inputs to subduction zones: Why lithostratigraphy and clay mineralogy matter, *in* Dixon, T.H., and Moore, J.C., eds., *The Seismogenic Zone of Subduction Thrust Faults*: New York, Columbia University Press, p. 42–85, <https://doi.org/10.7312/dixo13866-003>.

Vogt, C., Lauterjung, J., and Fischer, R., 2002, Investigation of the clay fraction (<2 μm) of the Clay Minerals Society reference clays: *Clays and Clay Minerals*, v. 50, p. 388–400, <https://doi.org/10.1346/00098600276083765>.

White, R., Spinelli, G.A., Mozley, P.S., and Dunbar, N.W., 2011, Importance of volcanic glass alteration to sediment stabilization: Offshore Japan: *Sedimentology*, v. 58, p. 1138–1154, <https://doi.org/10.1111/j.1365-3091.2010.01198.x>.

Printed in the USA